Applied Radiation and Isotopes 200 (2023) 110969

Contents lists available at ScienceDirect

Applied Radiation and Isotopes

journal homepage: www.elsevier.com/locate/apradiso

Experimental assessment of nuclear cross sections for the production of Tb radioisotopes with a medical cyclotron

Gaia Dellepiane [a,*], Pierluigi Casolaro [a], Alexander Gottstein [a], Isidre Mateu [a], Paola Scampoli [a,b], Saverio Braccini [a]

[a] Albert Einstein Center for Fundamental Physics (AEC), Laboratory for High Energy Physics (LHEP), University of Bern, Sidlerstrasse 5, CH-3012 Bern, Switzerland

[b] Department of Physics "Ettore Pancini", University of Napoli Federico II, Complesso Universitario di Monte S. Angelo, 80126 Napoli, Italy

ARTICLE INFO

Keywords:
Nuclear cross sections
Terbium-155
Data analysis
Medical cyclotron
Gadolinium targets
SPECT imaging
Theranostics

ABSTRACT

^{155}Tb is one of the most interesting radionuclides for theranostic applications. It is suitable for SPECT imaging and it can be used as a true diagnostic partner of the therapeutic ^{149}Tb and ^{161}Tb. Its production by proton irradiation using enriched ^{155}Gd and ^{156}Gd oxide targets is currently being investigated and represents a promising solution. To achieve the level of radionuclidic purity required in the clinical setting, the co-production of Tb impurities has to be minimized. For this purpose, an accurate knowledge of the cross sections of the nuclear reactions involved is of paramount importance. In this paper, we report on the assessment of cross sections of the reactions ^{154}Gd(p,xn)^{153,154,154m1,154m2}Tb, ^{155}Gd(p,xn)^{154,154m1,154m2,155}Tb, ^{156}Gd(p,xn)^{155,156}Tb and ^{157}Gd(p,2n)^{156}Tb derived with a specific data analysis procedure developed by our group. This method allows to disentangle the nuclear contributions from the production cross section by inverting linear systems of equations and it requires the measurement of the cross sections from as many materials as the reactions involved in the production of the radionuclide under study. For this purpose, the experimental data previously measured by our group at the Bern medical cyclotron by irradiating natural Gd_2O_3, enriched $^{155}Gd_2O_3$ and enriched $^{156}Gd_2O_3$ targets were used. For some of these nuclear reactions, cross sections were assessed for the first time. On the basis of our findings, production yield and purity can be calculated for any kind of isotopic composition of the enriched material.

1. Introduction

Along with the growth of theranostics and personalized nuclear medicine, terbium has attracted considerable interest because it offers four radioisotopes with complementary physics characteristics for medical applications: ^{149}Tb, ^{152}Tb, ^{155}Tb and ^{161}Tb (Müller et al., 2012).

^{152}Tb [$t_{1/2}$ = 17.5 h; EC, β^+: 100%] and ^{155}Tb [$t_{1/2}$ = 5.32 d; EC: 100%] (IAEA, 2021) are currently under investigation for PET and SPECT imaging, respectively, while ^{149}Tb [$t_{1/2}$ = 4.12 h; EC, β^+: 83.3%, α: 16.7%] and ^{161}Tb [$t_{1/2}$ = 6.95 d (Durán et al., 2020); β^-: 100%] (IAEA, 2021) are respectively α and β^- emitters suitable for radionuclide therapy.

Having identical chemical characteristics, terbium radioisotopes can be used to label radiopharmaceuticals that undergo the same metabolic processes, making it possible to predict whether a patient will benefit from a therapeutic treatment based on nuclear imaging data. For this to be possible, their availability in quantities and qualities suitable for medical application is of paramount importance.

In the case of diagnostic radionuclides, while the production of ^{152}Tb remains an open scientific challenge, several production routes for ^{155}Tb have been proposed in the literature (Dmitriev et al., 1989; Vermeulen et al., 2012; Steyn et al., 2014; Müller et al., 2014; Kazakov et al., 2018; Webster et al., 2021; Fiaccabrino et al., 2021). In particular, the production of high ^{155}Tb activities via proton irradiation of highly enriched ^{155}Gd and ^{156}Gd oxide targets and its subsequent radiochemical separation from the target material and impurities were reported by Favaretto et al. (2021). As part of the same project, a detailed study of the terbium radioimpurities produced in the irradiation was carried out to determine the optimal conditions for maximizing ^{155}Tb yield and radionuclidic purity (Dellepiane et al., 2022b). For this purpose, the production cross sections of terbium radioisotopes from natural Gd and enriched ^{155}Gd and ^{156}Gd oxide targets were measured at the Bern medical cyclotron laboratory, where an 18 MeV medical cyclotron is in operation (Braccini et al., 2011).

In the case of natural Gd_2O_3, our results were compatible with other experimental data reported in the literature (Vermeulen et al., 2012;

* Corresponding author.
E-mail address: gaia.dellepiane@lhep.unibe.ch (G. Dellepiane).

https://doi.org/10.1016/j.apradiso.2023.110969
Received 17 May 2023; Received in revised form 12 July 2023; Accepted 31 July 2023
Available online 2 August 2023

Table 1
Physical properties and main γ-emissions of the investigated Tb radioisotopes (IAEA, 2021). BR is the branching ratio of the γ-line. The values in brackets are the uncertainties referred to the last digits of the value.

Radioisotope	Nuclear reactions	Half-life	Decay mode: (%)	E_γ (keV)	BR_γ (%)
^{153}Tb	^{154}Gd(p,2n) + ^{155}Gd(p,3n)	2.34*(1)* d	EC, β^+: 100	212.00*(2)*	28.5*(19)*
^{154}Tb	^{154}Gd(p,n) + ^{155}Gd(p,2n)	21.5*(4)* h	EC, β^+: 100	1291.31*(13)*	6.9*(5)*
^{154m1}Tb	^{154}Gd(p,n) + ^{155}Gd(p,2n)	9.4*(4)* h	EC, β^+: 78.2 IT: 21.8	540.18*(6)* –	20*(3)* –
^{154m2}Tb	^{154}Gd(p,n) + ^{155}Gd(p,2n)	22.7*(5)* h	EC, β^+: 98.2 IT: 1.8	426.78*(7)* –	17.3*(12)* –
^{155}Tb	^{155}Gd(p,n) + ^{156}Gd(p,2n) + ^{157}Gd(p,3n)	5.32*(6)* d	EC: 100	105.318*(3)*	25.1*(13)*
^{156}Tb	^{156}Gd(p,n) + ^{157}Gd(p,2n)	5.35*(10)* d	EC, β^+: 100	534.29*(6)*	67*(6)*
^{156m1}Tb	^{156}Gd(p,n) + ^{157}Gd(p,2n)	24.4*(10)* h	IT: 100	–	–
^{156m2}Tb	^{156}Gd(p,n) + ^{157}Gd(p,2n)	5.3*(2)* h	IT: 100	–	–

Table 2
Isotopic compositions of the natural Gd oxide powder purchased by GoodFellow (https://www.goodfellow.com/) and of the enriched ^{155}Gd and ^{156}Gd oxide powders purchased from Isoflex (http://www.isoflex.com/). The values in brackets are the uncertainties referred to the last digits of the value.

	^{152}Gd	^{154}Gd	^{155}Gd	^{156}Gd	^{157}Gd	^{158}Gd	^{160}Gd
Natural (%)	0.20	2.18	14.80	20.47	15.65	24.84	21.86
^{155}Gd-enr. (%)	<0.02	0.5	91.90*(30)*	5.87	0.81	0.65	0.27
^{156}Gd-enr. (%)	<0.01	0.05	0.87	93.30*(10)*	4.38	1.08	0.32

Table 3
^{154}Gd(p,2n)^{153}Tb and ^{155}Gd(p,3n)^{153}Tb reaction cross sections.

E (MeV)	^{154}Gd(p,2n)^{153}Tb (mbarn)	^{155}Gd(p,3n)^{153}Tb (mbarn)
11.5 ± 0.4	–	–
11.9 ± 0.4	181 ± 45	–
12.1 ± 0.4	194 ± 52	–
13.0 ± 0.4	358 ± 33	–
14.5 ± 0.4	528 ± 44	–
15.8 ± 0.4	648 ± 51	–
17.1 ± 0.4	901 ± 72	–
18.2 ± 0.4	1098 ± 118	5 ± 2

Challan et al., 2007). In the case of the enriched materials, however, it was not possible to make a comparison with the results obtained by other groups (Dmitriev et al., 1989) due to differences in the isotopic abundance of the irradiated materials. In fact, since all Tb radioisotopes are produced by more than one nuclear reaction in the energy range of interest (Table 1), the assessment of the nuclear contributions from the production cross sections is challenging. For this purpose, our group developed a specific data analysis procedure (Braccini et al., 2022; Dellepiane et al., 2022a). This method requires to measure the cross sections from as many materials with different isotopic compositions as the reactions involved in the production of the radionuclide under study, and it allows to disentangle the nuclear contributions from the production cross section.

The aim of this study was to assess the cross section of the nuclear reactions involved in producing terbium radioisotopes from Gd_2O_3 target irradiations, applying the new analysis method to the data already published in Ref. Dellepiane et al. (2022b).

The knowledge of the nuclear cross sections is important since it makes possible to determine the expected ^{155}Tb production yield and radionuclidic purity for any isotopic composition of the enriched Gd_2O_3 target used.

2. Material and methods

The data analyzed in this paper were measured at the Bern medical cyclotron (Dellepiane et al., 2022b) by irradiating natural Gd and highly enriched ^{155}Gd and ^{156}Gd oxide targets (isotopic composition in Table 2) with an experimental procedure developed by our group (Carzaniga et al., 2017). This method is based on the irradiation of the full mass of a thin target by a proton beam with a constant surface distribution and has the advantage that the target has not to be necessarily uniform in thickness, provided that the energy of the protons can be considered constant within its mass.

To perform irradiations below 18 MeV, the beam energy was degraded by means of aluminium attenuator discs placed in front of the target and was determined using the SRIM-2013 Monte Carlo code.

Since all Tb radioisotopes are produced by at least two nuclear reactions in the energy range of interest (Table 1), a method based on the inversion of a linear system of equations was applied to disentangle the nuclear contributions from the production cross sections.

Considering two materials A and B with different known isotopic compositions, in the case of two reactions (p,x) and (p,y) starting from the ith and jth isotope, respectively, the following linear system holds for a given beam energy:

$$\begin{cases} \sigma^A_{TOT} = \beta^A_i \cdot \sigma(p,x) + \beta^A_j \cdot \sigma(p,y) \\ \sigma^B_{TOT} = \beta^B_i \cdot \sigma(p,x) + \beta^B_j \cdot \sigma(p,y) \end{cases} \quad (1)$$

where the experimentally measured production cross sections appear on the left side of the equations and the reaction cross sections to be determined on the right. $\beta^{A,B}_{i,j}$ is the abundance of the target isotope in the considered material.

The uncertainties of the nuclear cross sections were derived by considering the maximum and minimum value of the production cross sections.

The isotopic abundances of Gd isotopes are considered error-free, except for enrichment isotopes for which the uncertainty is provided by the manufacturer.

3. Data analysis and results

Terbium-153

In the investigated energy region, ^{153}Tb is mainly produced from ^{154}Gd and ^{155}Gd via the reactions (p,2n) and (p,3n), respectively. The latter has a threshold energy of about 18 MeV and was only observed for the maximum reachable energy. The calculated nuclear cross sections are presented in Fig. 1 and the numerical data are given in the Appendix (Table 3). Our results are well reproduced by the TENDL-2021 (Koning and Rochman, 2012) calculations. To the best of our knowledge, no experimental data are available in the literature.

Terbium-154, terbium-154m1 and terbium-154m2

Three isomers of ^{154}Tb (ground state, m1 and m2) are produced in the energy range of interest by the ^{154}Gd(p,n) ^{154x}Tb and ^{155}Gd(p,2n)^{154x}Tb reactions. The threshold energy of the latter lies at about 10.5 MeV.

The m1 state decays through EC (78%) and IT (22%) into ^{154}Gd and the ground state of ^{154}Tb, respectively. The m2 state decays mainly through EC (98%) into ^{154}Gd. In our previous publication (Dellepiane et al., 2022b), we proved that the contributions of the metastable states

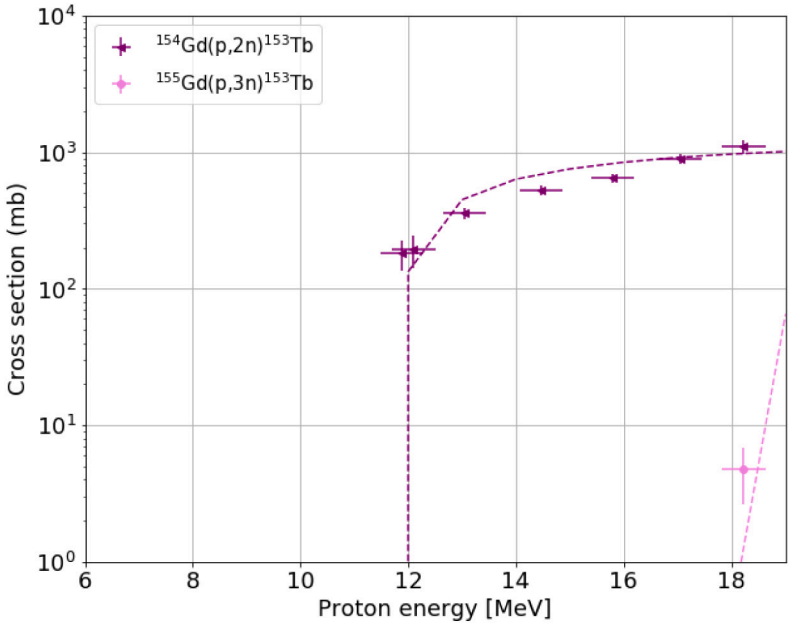

Fig. 1. ^{154}Gd(p,2n)^{153}Tb and ^{155}Gd(p,3n)^{153}Tb reaction cross sections. The dots are the experimental points, the dashed lines are the TENDL calculations.

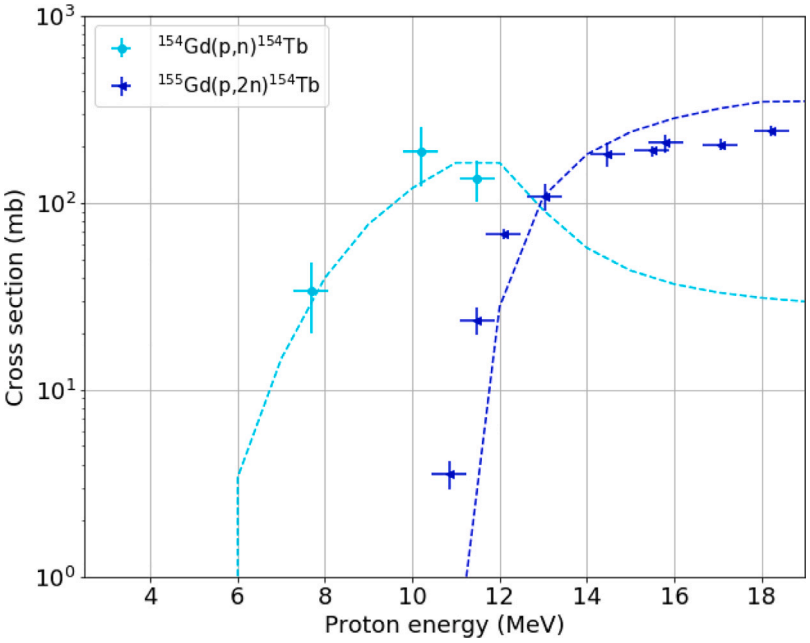

Fig. 2. ^{154}Gd(p,n)^{154}Tb and ^{155}Gd(p,2n)^{154}Tb reaction cross sections. The dots are the experimental points, the dashed lines are the TENDL calculations.

to the activity of the ground state are negligible, thus each isomer can be considered separately.

The nuclear cross sections are presented in Figs. 2–4 and the numerical data are given in the Appendix (Tables 4–6). In both cases, it was possible to calculate the cross sections of the ^{154}Gd(p, (n) ^{154x}Tb reaction only for energies below 10.5 MeV. Above this value, the contribution of the ^{155}Gd(p,2n) reaction is strongly predominant for all three investigated materials.

Terbium-155

In the investigated energy region, ^{155}Tb is mainly produced by the reactions ^{155}Gd(p,n), ^{156}Gd(p,2n) and ^{157}Gd(p,3n). The last two reactions have threshold energies at about 11 MeV and 17 MeV, respectively.

In order to disentangle the three contributions, the production cross sections measured from natural gadolinium oxide (Table 2) were also considered.

The nuclear cross sections are presented in Fig. 5 and the numerical data are reported in the Appendix (Table 7). In all three cases, the TENDL calculations generally reproduce our data very well. The discrepancy observed at around 13 MeV may be attributed to a limitation of the analysis method used in this work, as the investigated cross sections are nearly equivalent at that energy.

To the best of our knowledge, no experimental data are available in the literature.

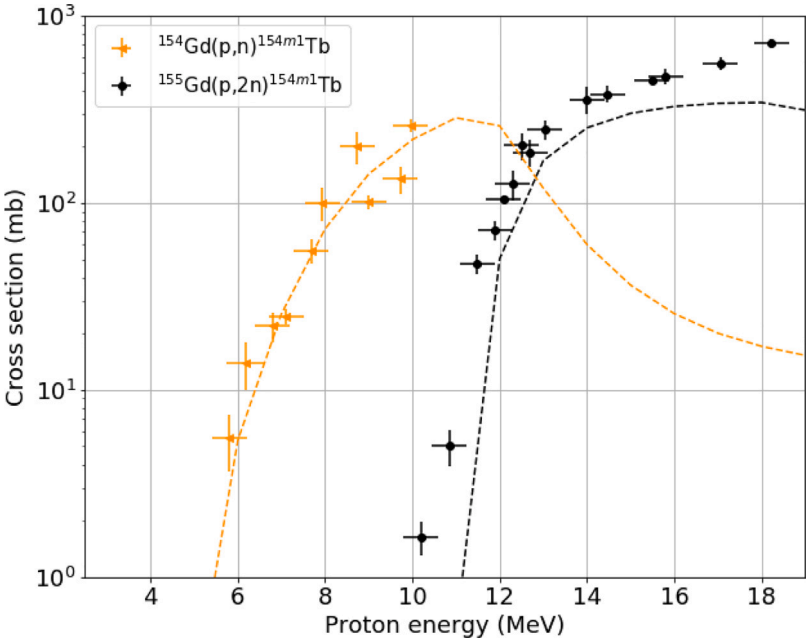

Fig. 3. ^{154}Gd(p,n) ^{154m1}Tb and ^{155}Gd(p,2n)^{154m1}Tb reaction cross sections. The dots are the experimental points, the dashed lines are the TENDL calculations.

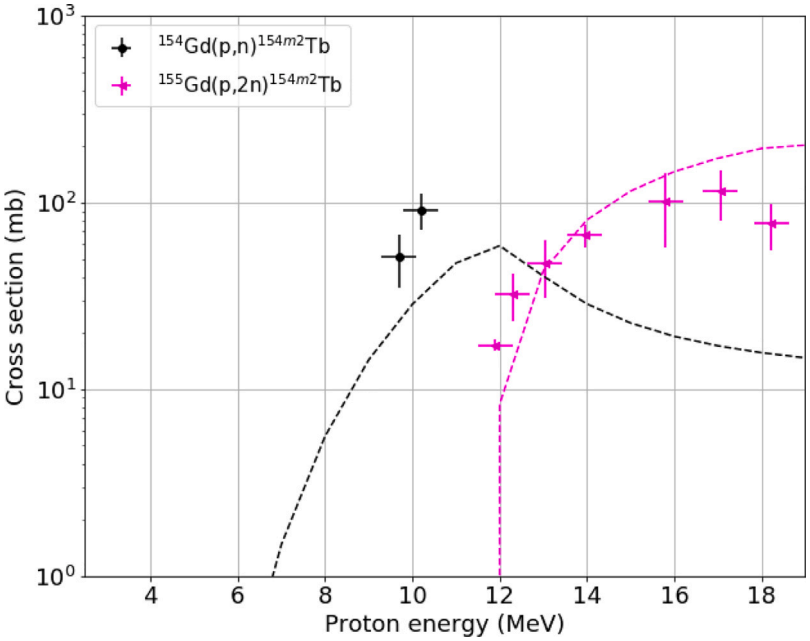

Fig. 4. ^{154}Gd(p,n) ^{154m2}Tb and ^{155}Gd(p,2n)^{154m2}Tb reaction cross sections. The dots are the experimental points, the dashed lines are the TENDL calculations.

Terbium-156

Three isomers of ^{156}Tb (ground state, m1 and m2) are produced in the energy range of interest mainly by the ^{156}Gd(p, (n) ^{156x}Tb and ^{157}Gd(p,2n)^{156x}Tb reactions. The threshold energy of the latter lies at about 10 MeV. Both the m1 and m2 states decays through IT (100%) into the ground state, causing an increase in its activity, without any γ-ray emission.

In our previous publication (Dellepiane et al., 2022b), we evaluated the production cross sections of the three isomers using a method based on repeated measurements of the samples over time. We also determined the ^{156}Tb cumulative cross section by measuring the samples after a sufficiently long time to have the metastable states decayed.

Only the latter data were re-analyzed in this paper to assess nuclear cross sections, due to the larger number of measurements and greater relevance in the ^{155}Tb production for medical applications.

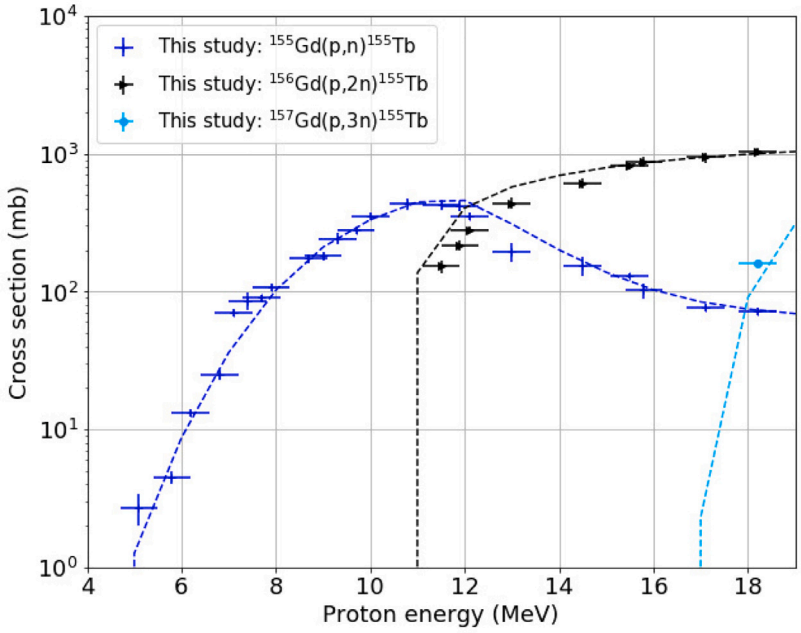

Fig. 5. ^{155}Gd(p,n)^{155}Tb, ^{156}Gd(p,2n)^{155}Tb and ^{157}Gd(p,3n)^{155}Tb reaction cross sections. The dots are the experimental points, the dashed lines are the TENDL calculations.

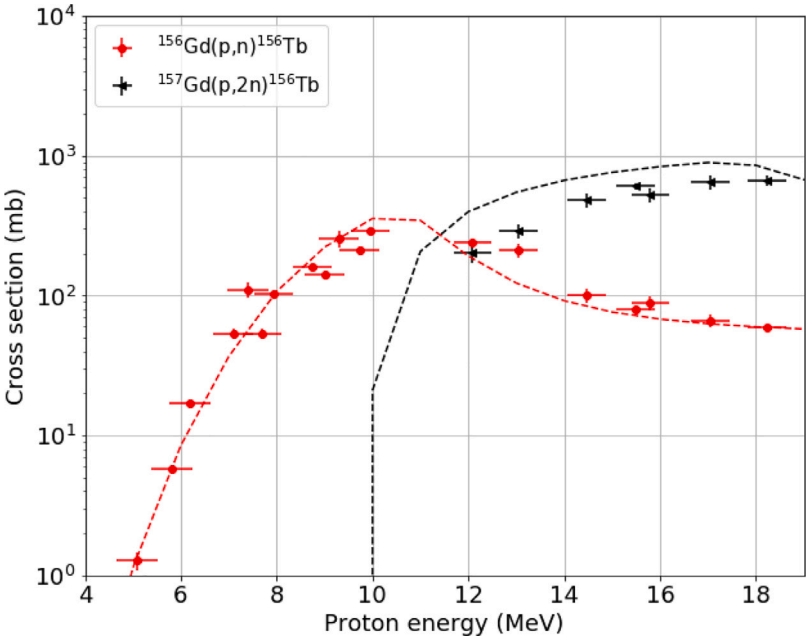

Fig. 6. ^{156}Gd(p,n)^{156}Tb and ^{157}Gd(p,2n)^{156}Tb reaction cross sections. The dots are the experimental points, the line dashed lines are the TENDL calculations.

Table 4
^{154}Gd(p,n)^{154}Tb and ^{155}Gd(p,2n)^{154}Tb reaction cross sections.

E (MeV)	^{154}Gd(p,n)^{154}Tb (mbarn)	^{155}Gd(p,2n)^{154}Tb (mbarn)
7.7 ± 0.4	34 ± 14	–
10.2 ± 0.4	189 ± 66	–
11.5 ± 0.4	135 ± 33	24 ± 4
12.1 ± 0.4	–	68 ± 4
13.0 ± 0.4	–	108 ± 18
14.5 ± 0.4	–	183 ± 26
15.5 ± 0.4	–	190 ± 12
15.8 ± 0.4	–	209 ± 24
17.1 ± 0.4	–	205 ± 14
18.2 ± 0.4	–	243 ± 15

Table 5
^{154}Gd(p,n)^{154m1}Tb and ^{155}Gd(p,2n)^{154m1}Tb reaction cross sections.

E (MeV)	^{154}Gd(p,n)^{154m1}Tb (mbarn)	^{155}Gd(p,2n)^{154m1}Tb (mbarn)
5.8 ± 0.4	6 ± 2	–
6.2 ± 0.4	14 ± 4	–
6.8 ± 0.4	22 ± 4	–
7.1 ± 0.4	25 ± 2	–
7.7 ± 0.4	56 ± 8	–
7.9 ± 0.4	100 ± 20	–
8.7 ± 0.4	200 ± 40	–
9.0 ± 0.4	101 ± 9	–
9.7 ± 0.4	134 ± 22	–
10.0 ± 0.4	260 ± 20	–
10.2 ± 0.4	–	1.6 ± 0.3
10.8 ± 0.4	–	5 ± 1
11.5 ± 0.4	–	47 ± 6
11.9 ± 0.4	–	71 ± 8
12.1 ± 0.4	–	104 ± 5
12.3 ± 0.4	–	126 ± 23
12.5 ± 0.4	–	203 ± 34
12.7 ± 0.4	–	186 ± 32
13.0 ± 0.4	–	247 ± 28
14.0 ± 0.4	–	356 ± 57
14.5 ± 0.4	–	381 ± 39
15.5 ± 0.4	–	452 ± 19
15.8 ± 0.4	–	475 ± 46
17.1 ± 0.4	–	557 ± 42
18.2 ± 0.4	–	721 ± 31

Table 6
^{154}Gd(p,n)^{154m2}Tb and ^{155}Gd(p,2n)^{154m2}Tb reaction cross sections.

E (MeV)	^{154}Gd(p,n)^{154m2}Tb (mbarn)	^{155}Gd(p,2n)^{154m2}Tb (mbarn)
9.7 ± 0.4	51 ± 16	–
10.2 ± 0.4	91 ± 20	–
11.5 ± 0.4	–	–
11.9 ± 0.4	–	17 ± 1
12.3 ± 0.4	–	32 ± 9
13.0 ± 0.4	–	47 ± 16
14.0 ± 0.4	–	67 ± 9
15.8 ± 0.4	–	101 ± 44
17.1 ± 0.4	–	115 ± 34
18.2 ± 0.4	–	77 ± 22

The results are presented in Fig. 6 and the numerical data are given in the Appendix (Table 8). For the ^{156}Gd(p,n)^{156}Tb reaction, TENDL predictions are in reasonable agreement with our findings, whereas for the ^{157}Gd(p,2n)^{156}Tb reaction a small overestimation can be observed.

4. Conclusions and outlook

Precise knowledge of the cross sections of nuclear reactions allows to determine the producible radionuclide activity and purity. When the radioisotope is produced by more than one reaction, decoupling the nuclear contributions from the production cross section is complicated and requires special data analysis procedures. For this purpose, our group has developed a method based on the inversion of linear systems of equations, which requires the measurement of cross sections from as many materials with different isotopic composition as the number of reactions involved in the production of the radionuclide under study.

This method was applied to the terbium radioisotope production cross sections previously measured by our group at the Bern medical cyclotron by irradiating natural Gd_2O_3, enriched $^{155}Gd_2O_3$ and enriched $^{156}Gd_2O_3$ targets. To the best of our knowledge, no other experimental data are reported in the literature for the reactions and energy range considered.

The results reported in this paper allow to calculate the ^{155}Tb production yield and the purity for any kind of enriched material and contribute to optimizing the production of ^{155}Tb for theranostics in nuclear medicine by irradiating Gd targets with medical cyclotrons.

Table 7
^{155}Gd(p,n)^{155}Tb, ^{156}Gd(p,2n)^{155}Tb and ^{157}Gd(p,3n)^{155}Tb reaction cross sections.

E (MeV)	^{155}Gd(p,n)^{155}Tb (mbarn)	^{156}Gd(p,2n)^{155}Tb (mbarn)	^{157}Gd(p,3n)^{155}Tb (mbarn)
5.1 ± 0.4	2.7 ± 0.7	–	–
5.8 ± 0.4	4.5 ± 0.5	–	–
6.2 ± 0.4	13.1 ± 0.8	–	–
6.8 ± 0.4	25 ± 2	–	–
7.1 ± 0.4	71 ± 5	–	–
7.4 ± 0.4	86 ± 13	–	–
7.7 ± 0.4	90 ± 5	–	–
7.9 ± 0.4	108 ± 7	–	–
8.7 ± 0.4	174 ± 12	–	–
9.0 ± 0.4	182 ± 14	–	–
9.3 ± 0.4	242 ± 23	–	–
9.7 ± 0.4	280 ± 18	–	–
10.0 ± 0.4	350 ± 22	–	–
10.8 ± 0.4	431 ± 38	–	–
11.5 ± 0.4	428 ± 39	153 ± 16	–
11.9 ± 0.4	418 ± 39	218 ± 19	–
12.1 ± 0.4	351 ± 23	281 ± 15	–
13.0 ± 0.4	194 ± 31	439 ± 40	–
14.5 ± 0.4	154 ± 25	616 ± 53	–
15.5 ± 0.4	130 ± 6	820 ± 42	–
15.8 ± 0.4	102 ± 13	872 ± 76	–
17.1 ± 0.4	76 ± 5	943 ± 78	–
18.2 ± 0.4	72 ± 5	1035 ± 65	161.5 ± 0.4

Table 8
^{156}Gd(p,n)^{156}Tb and ^{157}Gd(p,2n)^{156}Tb reaction cross sections.

E (MeV)	^{156}Gd(p,n)^{156}Tb (mbarn)	^{157}Gd(p,2n)^{156}Tb (mbarn)
5.1 ± 0.4	1.3 ± 0.2	–
5.8 ± 0.4	5.8 ± 0.4	–
6.2 ± 0.4	17 ± 1	–
7.1 ± 0.4	54 ± 5	–
7.4 ± 0.4	111 ± 14	–
7.7 ± 0.4	53 ± 4	–
7.9 ± 0.4	103 ± 5	–
8.7 ± 0.4	160 ± 11	–
9.0 ± 0.4	142 ± 10	–
9.3 ± 0.4	256 ± 34	–
9.7 ± 0.4	211 ± 15	–
10.0 ± 0.4	289 ± 10	–
12.1 ± 0.4	241 ± 11	202 ± 30
13.0 ± 0.4	209 ± 24	288 ± 32
14.5 ± 0.4	101 ± 11	482 ± 55
15.5 ± 0.4	80 ± 5	605 ± 32
15.8 ± 0.4	89 ± 10	522 ± 57
17.1 ± 0.4	66 ± 7	648 ± 74
18.2 ± 0.4	60 ± 3	670 ± 54

CRediT authorship contribution statement

Gaia Dellepiane: Writing – review & editing, Writing – original draft, Visualization, Validation, Software, Methodology, Investigation, Formal analysis, Data curation, Conceptualization. **Pierluigi**

Casolaro: Writing – review & editing, Investigation, Conceptualization. **Alexander Gottstein:** Writing – review & editing, Methodology. **Isidre Mateu:** Writing – review & editing, Methodology. **Paola Scampoli:** Writing – review & editing, Conceptualization. **Saverio Braccini:** Writing – review & editing, Supervision, Resources, Project administration, Methodology, Investigation, Funding acquisition.

Declaration of competing interest

The authors declare the following financial interests/personal relationships which may be considered as potential competing interests: Saverio Braccini reports financial support was provided by Swiss National Science Foundation.

Data availability

Data will be made available on request

Acknowledgments

This research project was partially funded by the Swiss National Science Foundation (SNSF) (grants: CRSII5_180352 and 200021_175749).

Appendix

See Tables 3–8.

References

Braccini, S., Carzaniga, T.S., Dellepiane, G., Grundler, P.V., Scampoli, P., van der Meulen, N.P., Wüthrich, D., 2022. Optimization of ^{68}Ga production at an 18 MeV medical cyclotron with solid targets by means of cross-section measurement of ^{66}Ga, ^{67}Ga and ^{68}Ga. Appl. Radiat. Isot. 186, 110252. http://dx.doi.org/10.1016/j.apradiso.2022.110252.

Braccini, S., Ereditato, A., Scampoli, P., von Bremen, K., 2011. The new Bern cyclotron laboratory for radioisotope production and research. In: Conf. Proc. C-IPAC-2011-THPS080, Vol. 110904. pp. 3619–3621.

Carzaniga, T.S., Auger, M., Braccini, S., Bunka, M., Ereditato, A., Nesteruk, K.P., Scampoli, P., Türler, A., van der Meulen, N.P., 2017. Measurement of ^{43}Sc and ^{44}Sc production cross-section with an 18 MeV medical PET cyclotron. Appl. Radiat. Isot. 129, 96–102. http://dx.doi.org/10.1016/j.apradiso.2017.08.013.

Challan, M.B., Moawadb, G.S., Abou-Zeidc, M.A., Comsana, M.N.H., 2007. Excitation functions of radionuclides produced by proton induced reactions on gadolinium targets. In: Proceedings of the 6th conference on nuclear and particle physics. Luxor, Egypt.

Dellepiane, G., Casolaro, P., Favaretto, C., Grundler, P.V., Mateu, I., Scampoli, P., Talip, Z., van der Meulen, N.P., Braccini, S., 2022b. Cross section measurement of terbium radioisotopes for an optimized ^{155}Tb production with an 18 MeV medical PET cyclotron. Appl. Radiat. Isot. 184, 110175. http://dx.doi.org/10.1016/j.apradiso.2022.110175.

Dellepiane, G., Casolaro, P., Mateu, I., Scampoli, P., Voeten, N., Braccini, S., 2022a. ^{47}Sc and ^{46}Sc cross-section measurement for an optimized ^{47}Sc production with an 18 MeV medical PET cyclotron. Appl. Radiat. Isot. 189, 110428. http://dx.doi.org/10.1016/j.apradiso.2022.110428.

Dmitriev, P.P., Molin, G.A., Dmitrieva, Z.P., 1989. Production of ^{155}Tb for nuclear medicine by reactions ^{155}Gd(p,n), ^{156}Gd(p,2n), ^{155}Gd(d2n). Atomnaya Ehnergiya 66, 419–421.

Durán, M.T., Juget, F., Nedjadi, Y., Bochud, F., Grundler, P.V., Gracheva, N., Müller, C., Talip, Z., van der Meulen, N.P., Bailat, C., 2020. Determination of ^{161}Tb half-life by three measurement methods. Appl. Radiat. Isot. 159, 109085. http://dx.doi.org/10.1016/j.apradiso.2020.109085.

Favaretto, C., Talip, Z., Borgna, F., Grundler, P., Dellepiane, G., Sommerhalder, A., Zhang, H., Schibli, R., Braccini, S., Müller, C., van der Meulen, N.P., 2021. Cyclotron production and radiochemical purification of terbium-155 for SPECT imaging. EJNMMI Radiopharm. Chem. 6, 37. http://dx.doi.org/10.1186/s41181-021-00153-w.

Fiaccabrino, D.E., Kunz, P., Radchenko, V., 2021. Potential for production of medical radionuclides with on-line isotope separation at the ISAC facility at TRIUMF and particular discussion of the examples of ^{165}Er and ^{155}Tb. Nucl. Med. Biol. 94–95, 81–91. http://dx.doi.org/10.1016/j.nucmedbio.2021.01.003.

IAEA, 2021. Live chart of nuclides. available online, URL https://nds.iaea.org/relnsd/vcharthtml/VChartHTML.html, Last access 27 December 2021.

Kazakov, A.G., Aliev, R.A., Bodrov, A.Y., Priselkova, A.B., Kalmykov, S.N., 2018. Separation of radioisotopes of terbium from a europium target irradiated by 27 MeV α-particles. Radiochim. Acta 106 (2), 135–140. http://dx.doi.org/10.1515/ract-2017-2777.

Koning, A.J., Rochman, D., 2012. Modern nuclear data evaluation with the TALYS code system. Nucl. Data Sheets 113, http://dx.doi.org/10.1016/j.nds.2012.11.002, 2841–2934.

Müller, C., Fischer, E., Behe, M., Koster, U., Dorrer, H., Reber, J., Haller, S., Cohrs, S., Blanc, A., Grunberg, J., Bunka, M., Zhernosekov, K., van der Meulen, N.P., Johnston, K., Turler, A., Schibli, R., 2014. Future prospects for SPECT imaging using the radiolanthanide terbium-155 — production and preclinical evaluation in tumor-bearing mice. Nucl. Med. Biol. 41, e58 – e65. http://dx.doi.org/10.1016/j.nucmedbio.2013.11.002.

Müller, C., Zhernosekov, K., Koster, U., Johnston, K., Dorrer, H., Hohn, A., van der Walt, N.T., Turler, A., Schibli, R., 2012. A unique matched quadruplet of terbium radioisotopes for PET and SPECT and for α^- and β^--radionuclide therapy: An in vivo proof-of-concept study with a new receptor-targeted folate derivative. J. Nucl. Med. 53, 1951–1959. http://dx.doi.org/10.2967/jnumed.112.107540.

Steyn, G.F., Vermeulen, C., Szelecsényi, F., Kovacs, Z., Hohn, A., van der Meulen, N.P., Schibli, R., van der Walt, T.N., 2014. Cross sections of proton-induced reactions on ^{152}Gd, ^{155}Gd and ^{159}Tb with emphasis on the production of selected Tb radionuclides. Nucl. Instrum. Methods Phys. Res. B 319, 128–140. http://dx.doi.org/10.1016/j.nimb.2013.11.013.

Vermeulen, C., Steyn, G.F., Szelecsényi, F., Kovacs, Z., Suzuki, K., Nagatsu, K., Fukumura, T., Hohn, A., van der Walt, T.N., 2012. Cross sections of proton-induced reactions on ^{nat}Gd with special emphasis on the production possibilities of ^{152}Tb and ^{155}Tb. Nucl. Instrum. Methods Phys. Res. B 275, 24–32. http://dx.doi.org/10.1016/j.nimb.2011.12.064.

Webster, B., Ivanov, P., Russell, B., Collins, S., Stora, T., Ramos, J.P., Köster, U., Robinson, A.P., Read, D., 2021. Chemical purification of terbium-155 from pseudo-isobaric impurities in a mass separated source produced at CERN. Sci. Rep. 9, 10884. http://dx.doi.org/10.1038/s41598-019-47463-3.